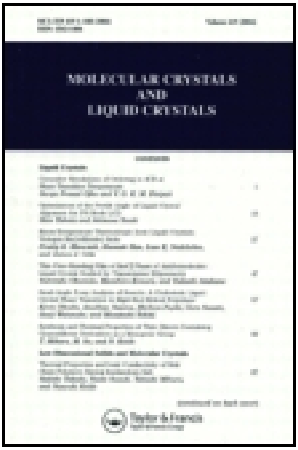

Molecular Crystals and Liquid Crystals
Publication details, including instructions for authors and subscription information:
http://www.tandfonline.com/loi/gmcl20

Effect of Recording Time on Grating Formation and Enhancement in an Amphiphilic Diblock Liquid-Crystalline Copolymer

Haifeng Yu* [a], Yumiko Naka [a], Atsushi Shishido [a], Tomokazu Iyoda [a] & Tomiki Ikeda [a]

[a] Chemical Resources Laboratory, Tokyo Institute of Technology, Midori-ku, Yokohama, Japan

To cite this article: Haifeng Yu*, Yumiko Naka, Atsushi Shishido, Tomokazu Iyoda & Tomiki Ikeda (2009): Effect of Recording Time on Grating Formation and Enhancement in an Amphiphilic Diblock Liquid-Crystalline Copolymer, Molecular Crystals and Liquid Crystals, 498:1, 29-39

To link to this article: http://dx.doi.org/10.1080/15421400802612094

Mol. Cryst. Liq. Cryst., Vol. 498, pp. 29–39, 2009
Copyright © Taylor & Francis Group, LLC
ISSN: 1542-1406 print/1563-5287 online
DOI: 10.1080/15421400802612094

Effect of Recording Time on Grating Formation and Enhancement in an Amphiphilic Diblock Liquid-Crystalline Copolymer

Haifeng Yu*, **Yumiko Naka, Atsushi Shishido, Tomokazu Iyoda, and Tomiki Ikeda**
Chemical Resources Laboratory, Tokyo Institute of Technology,
Midori-ku, Yokohama, Japan

To precisely control the first-order diffraction efficiency of holographic gratings recorded in an amphiphilic diblock liquid-crystalline copolymer P40A37, effect of recording time on grating formation and enhancement was studied systematically. Several parameters such as surface relief, the first-order diffraction efficiency, the maximum transmittance under an optical polarizing microscope and order parameters of grating samples were evaluated before and after annealing. Then the enhancement coefficient with recording time was estimated. The best enhancement effect was obtained at 10-s recording upon nano-scaled phase separation. By precisely adjusting the recording time, the diffraction efficiency of holographic gratings in P40A37 can be finely controlled from 0.13% to 10%.

Keywords: amphiphilic diblock copolymer; azobenzene-containing liquid-crystalline polymer; diffraction efficiency; holographic grating; nano-scaled phase separation

INTRODUCTION

As one of the most promising candidate materials for holographic data storage, the chromophore-containing organic materials have attracted much attention of scientific researchers [1–11]. Among them, azobenzene (AZ)-containing liquid-crystalline polymers (LCPs), in which the AZ moiety plays both roles as a mesogen and a photosensitive chromophore [3,4], have been extensively studied because their large

---

Present address: Top runner incubation center for academia-industry fusion, Room 425, Department of Chemistry, Nagaoka University of Technology, 1603-1 Kamitomioka, Nagaoka 940-2188, Japan. E-mail: yuhaifeng@mst.nagaokaut.ac.jp

Address correspondence to Tomiki Ikeda, Chemical Resources Laboratory, Tokyo Institute of Technology, 21-11, 4259 Nagatsuta, Midori-ku, Yokohama 226-8503, Japan. E-mail: tikeda@res.titech.ac.jp

birefringence and optical anisotropy can be induced in grating recording process [5]. Generally, diffraction efficiency (DE) is one of the most important parameters in holographic gratings, which has been controlled by several methods. In addition to altering the chemical structures of polymers with AZ moieties in the side chain or main chain, other physical ways such as gain effects of partially crystalline or LC materials [6,7], mechanically-stretchable elastomers [8], electrically-switchable polymerized nematic emulsions [9], self-assembled LC gels [10], and mixture of low molecular-weight LCs [11] have been explored.

Recently, we reported a simple method of controlling the first-order DE by thermally-induced nano-scaled phase separation (NSPS) based on an amphiphilic diblock liquid-crystalline copolymer (ADLC), consisting of poly(ethylene oxide) (PEO) and polymethacrylate containing an AZ moiety in the side chain [12,13]. Unlike the general microphase separation of polymer blends, the phase in the ADLC is composed of nano-scaled domains, which might get rid of the scattering of visible light [14–15]. By the way of NSPS without additional writing beams, the first-order DE was increased by almost two orders of magnitude, which can be applied to secure information storage since the information cannot be easily read out at a lower DE without the thermal treatment. To get the information recorded in the materials, the grating samples should undergo NSPS process to enhance DE.

Besides material structures, there are many factors that influence DE of gratings recorded in AZ-containing LCPs, including photoisomerization [1], molecular aggregation, phase transition of LC to isotropic (I) phase [16,17], microphase separation [13], mass-transportation process [2,18]. Obviously, the recording time can affect all the above-mentioned aspects, which is worthy to be studied systematically. As reported previously [13], the selective cis-trans photoisomerization and I-LC phase transition as well as alignment of trans-AZ mesogens were induced by the interference pattern of two coherence laser beams in the pre-irradiated ADLC films. Both a refractive-index grating (RIG) and a surface-relief grating (SRG) contributed to DE generated in the recording process. Then a strong enhancement effect of the surface modulation was obtained owing to NSPS, which led to a drastic increase in DE. In this paper, we investigated the effect of recording time on the formation and enhancement of surface-relief and DE induced by the NSPS.

EXPERIMENTAL

Materials

As shown in Figure 1 (A), the ADLC P40A37 with a number-average molecular weight (Mn) of 18,700 and low polydispersity ($Mw/Mn = 1.09$),

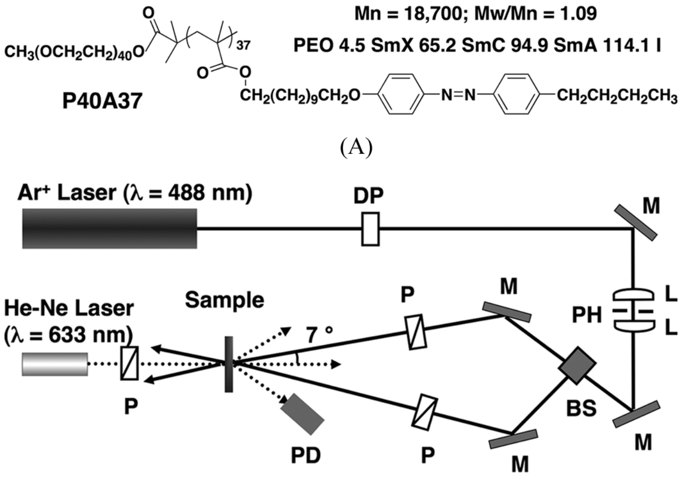

(A)

(B)

FIGURE 1 Materials and optical setup use in this paper for recording holographic gratings. (A) The chemical structure and properties materials (P40A37); (B) optical setup. BS, beam splitter; PD, photodiode; L, lens; M, mirror; P, polarizer; PH, pinhole; DP, depolarizer.

was used in this study. Four phase-transition peaks were obtained in its thermogram by differential scanning calorimetry at 4.5, 65.2, 94.9 and 114.1°C, corresponding to PEO melting point to smectic X to smectic C to smectic A to I phase, respectively. Two maximum absorption bands were observed in its UV-Vis spectrum in chloroform solution. One band around 350 nm is owing to the π-π^* transition, the other band at 450 nm is attributed to the n-π^* transition [1]. The PEO block is hydrophilic, whereas the AZ-containing polymethacrylate block is generally hydrophobic, which enables to form nano-scaled microphase-separated structures (PEO microphase domains with a cylinder of about 10 nm) by supramolecular self-assembly. The synthetic procedure and thermodynamic properties as well as the NSPS structures of P40A37 were reported elsewhere [12].

Characterization

^{1}H NMR spectra were measured using a Lambda-300 spectrometer operating at 300 Hz with tetramethylsilane as an internal reference for chemical shifts. The molecular weights of polymers were determined by gel permeation chromatography (GPC, JASCO) with standard polystyrenes in chloroform as eluent. The thermodynamic properties of the monomer and polymers were analyzed with a differential scanning calorimeter (DSC, Seiko) at a heating and cooling rate of 10°C/min. At least three scans were performed to check the reproducibility.

The copolymer films were prepared by spin-coating their toluene solutions on clean glass substrates. The film thickness was estimated about 600 nm with a surface profiler (Veeco Instruments Inc., Dektak 3ST), and the dimensionless Q-parameter of the films was about 0.37 according to the Eq. (1), which means that the recorded gratings belong to the Raman-Nath type.

$$Q = \frac{2\pi\lambda_R d}{n\Lambda^2} \tag{1}$$

where λ_R is the wavelength of the readout beam, d is the thickness of the film, n is the refractive index and Λ is the fringe spacing [19].

Both the LC behavior and the RIG structures were examined on a polarizing optical microscope (POM, Olympus Model BH-2). Unpolarized light at 366 nm was obtained from a 500 W high-pressure mercury lamp through three glass filters (Toshiba, UV-35, UV-D36A and IRA-25). UV-Vis spectra of the polymer in a chloroform solution or a spin-coated film were measured using a JASCO U-550 spectrometer. Atomic force microscopy (AFM) images of surface modulation in tapping mode were detected with a scanning probe microscope (Veeco Instruments Inc., Nanoscope IV) at room temperature.

Grating Recording and Enhancement

After pre-treatment upon irradiation with unpolarized 366-nm light, the holographic gratings were recorded on the P40A37 spin-coated films with the optical setup shown in Figure 1(B) by a standard procedure [5]. Two coherent s-polarized laser beams with equal intensity of 50 mW/cm^2 from an Ar$^+$ laser at 488 nm were crossed on the film surface at an incident angle of 7°, leading to an interference pattern with a fringe spacing of 2.0 μm according to $\Lambda = \lambda/(2\sin\theta)$, where λ and θ are the wavelength and the incident angle of the writing laser beams, respectively. The two beams were collimated to a diameter of about 2.0 mm on the film surface. A He-Ne laser beam (633 nm) with 10-W intensity was used as a reading beam since the copolymer films after pre-irradiation have little absorption at this wavelength [13]. The grating formation was confirmed in real time by monitoring the intensity of the first-order diffraction beam with a photodiode in a transmission mode, and the diffraction efficiency was defined as $\eta = I_1/I_0$, where I_1 is the intensity of the first-order diffraction beam, and I_0 represents the intensity of the transmitted beam through the film without the writing beams, respectively. The reading beam was also normally incident to the film surface.

After the grating formation at a certain recording time, a hot stage (METTLER TOLEDO FP 90 Central Processor) equipped with a METTLER FP 82 was used to heat the gating samples at a scanning rate of 1°C/min from 30°C to 100°C and annealed for 24 h. Then the grating samples were cooled to room temperature at 1°C/min. The change in structures of RIG and SRG was characterized by POM and AFM, respectively. The anisotropy of the sample films was measured by polarized UV-Vis spectra. The order parameter (S) can be calculated by Eq. (2),

$$S = (A_{\perp} - A_{||})/(A_{\perp} + 2A_{||}) \tag{2}$$

where $A_{\perp}$ and $A_{//}$ denote the absorption perpendicular and parallel to the grating vector, respectively [20].

RESULTS AND DISCUSSION

After the pre-treatment, holographic gratings were successfully recorded in the copolymer films. Both a RIG and a SRG were clearly observed as shown in Figure 2. The grating periods of the RIG and SRG were 2.0 µm, which are consistent with the calculated fringe spacing of the interference pattern. Table 1 summarizes the corresponding grating structures in the POM and AFM images. The bright areas of the interference pattern correspond to the valleys of the SRG (the bright stripes of the RIG images), whereas the dark areas are correlated with the peaks of the SRG (the dark stripes of the RIG images),

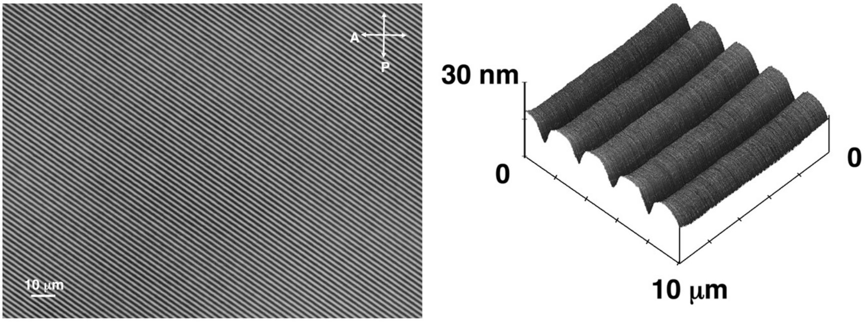

(A) (B)

FIGURE 2 Typical structures of holographic gratings recorded at 10 s in the copolymer films. (A) RIG, P, polarizer; A, analyzer; (B) SRG.

TABLE 1 Summary of Holographic Grating zStructures in POM and AFM Images

Phase state	RIG (POM)	SRG (AFM)
I	Dark stripe	Peak
LC	Bright stripe	Valley

which is contrary to our previous results of AZ-containing LCPs since the pre-treatment was performed beforehand to induce a cis-AZ-rich I phase in the ADLC films [5]. Both the SRG and RIG structures were stable under room light.

The growth of the surface relief and DE of the gratings with recording time are shown in Figure 3(A). Upon irradiation with two coherent laser beams, DE increased sharply at the early stage, gradually reached the maximum about 0.13% at 10 s, and then slowly decreased with a longer recording time. Different from the diffraction behavior, the surface relief of the gratings never showed any decrease with recording time. It increased quickly to 16.8 nm at 10 s, and then grew very slowly to about 18 nm at 40 s.

After the grating formation, the LC alignment in the irradiated areas was checked by measuring the transmittance (T), placing sample films between a set of two-crossed polarizer and analyzer, as a function of rotation angle between the grating vector and the polarizer. The angular-dependent T of the grating areas exhibited a standard sinusoidal curve with a periodicity of 90°, indicating that the AZ mesogens in the bright stripes under a POM are

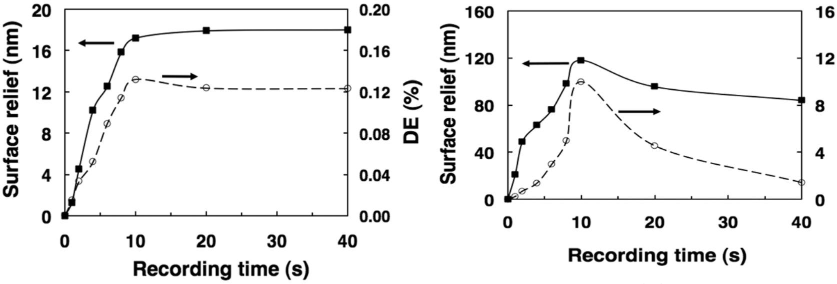

(A) (B)

FIGURE 3 The growth of surface relief and the first-order DE with recording time before (A) and after (B) annealing. DE, the first-order diffraction efficiency.

homogenously aligned, perpendicular to the polarization direction of writing beams according to the Weigert effect [21]. Figure 4(A) gives the dependence of the maximum T (T_{max}) of the grating samples on recording time. T_{max} increased gradually with recording time, showing that the LC alignment in the bright stripes was improved with an increase in recording time. The value of S in grating samples with recording time showed the similar behavior to those of the T_{max}. After recording for 40 s, the S of about 0.035 was obtained, with the T_{max} of about 13%.

Then all the grating samples were annealed to obtain the enhancement effect in the absence of the writing beams. As shown in Figure 3 (B), all the recorded gratings exhibited a drastic increase in both the surface modulation and DE. At 10-s recording, the maximum value of about 120 nm in surface relief and 10% in DE were obtained, respectively. The similar enhancement was observed for the gratings recorded within 40 s. They increased up to 10 s, and then decreased slowly passing the critical point. The enhancement effect might be ascribed to the different pressure (ΔP) between bright stripes and dark stripes in POM pictures of gratings produced by the NSPS [13], which is different from other enhancement mechanisms explained by either improved LC alignment or selective crystallization [6,7]. The PEO blocks have better compatibility with I polymer blocks in the dark area than the LCP blocks in the bright area after grating recording. Thus better NSPS can be obtained in the bright stripes upon annealing, inducing higher pressure in the bright stripes compared to the dark areas, which leads to the uplift of the dark stripes (the peaks of the SRG). Furthermore, the I state can

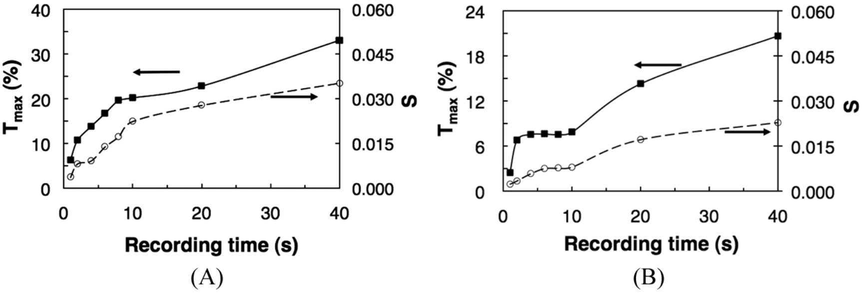

(A) (B)

FIGURE 4 Change in T_{max} and S of the grating areas with recording time before (A) and after (B) annealing. T_{max}, the maximum transmittance of the grating samples between a set of two-crossed polarizer and analyzer; S, order parameter.

improve the molecular mobility of the ADLC films, which enables the mass transportation to form the surface-relief enhancement. Obviously, the higher the ΔP induced by the NSPS, the stronger the enhancement effect caused. As a result of the higher surface relief, a larger DE of the grating was obtained.

Within a short recording time (<10 s), the LC content in the bright stripes triggered by the writing beams increased with a recording time, which would produce higher ΔP and a resultant higher surface relief upon annealing. When a high LC ratio in the bright stripes was obtained, several disadvantages to the enhancement were observed. Firstly, a higher writing energy dose may induce generation of a partial LC phase in the dark stripes of the grating samples, which can decrease the difference in refractive index between the dark and bright stripes, leading to a lower DE (longer than 10 s). Secondly, stronger H-aggregates of AZ might be formed during the annealing process when the LC content is relatively high, disturbing the LC alignment and reducing the birefringence in the bright stripes [13]. Thirdly, the self-organization (or cooperative motion) of the LC molecules can destroy the interface between the bright and dark stripes, leading to the deformation of the stripes in the POM images shown in Figure 5. Although the RIG structures remained after annealing,

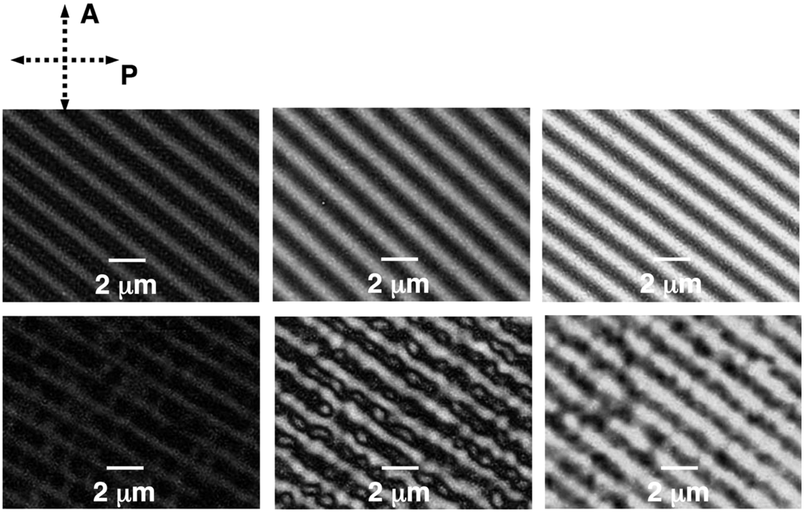

FIGURE 5 POM images of RIGs before (above) and after (below) annealing. The gratings were recorded for 2 s, 10 s and 40 s, respectively. P and A are polarizer and analyzer of the POM, respectively.

the interface between the bright and dark stripes in the POM pictures became fuzzy. Furthermore, the annealed grating samples showed darker images than those before annealing, which might originate from the variation in the LC alignment during the annealing process. Unlike the bright stripes, the dark stripes in the cis-AZ-rich I phase showed different behavior. After annealing, a part of cis-AZs thermally isomerized to trans-AZ mesogens, but the dark stripes were still observed in Figure 5. Thus the molecular cooperative motions of the LCs with different alignment directions between the bright and dark stripes should be induced because of the LC inherent properties [3], which disturbed the edge of the two areas and resulted in the ambiguous interface in AFM images (Fig. 6). Fourthly, the NSPS process involves not only molecular mass transportation but also the partial disturbance of LC alignment in the bright stripes. Therefore, the enhancement effect was weakened by the above-mentioned demerits with a longer recording time (>10 s). Since both the H-aggregation and the mass transportation were induced in the NSPS process, the LC alignment pre-orientated by the polarized writing beams was disturbed partly, which led to the decrease in both T_{max} and S shown in Figure 4(B).

To qualitatively characterize the enhancement effect on recording time, the enhancement coefficient (EC) was defined as

$$EC = \eta_A/\eta_B \qquad (3)$$

where η_B and η_A are the first-order DE of the gratings before and after NSPS upon annealing, respectively. As shown in Figure 7, the EC

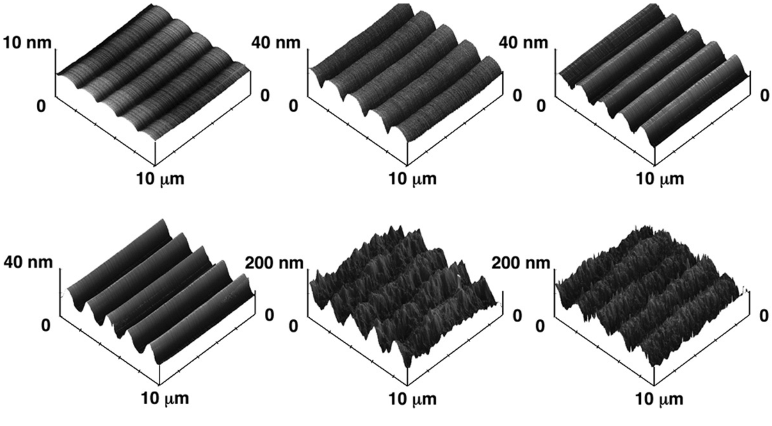

FIGURE 6 3D AFM pictures of SRGs before (above) and after (below) annealing. The gratings were recorded at 2 s, 10 s and 40 s, respectively.

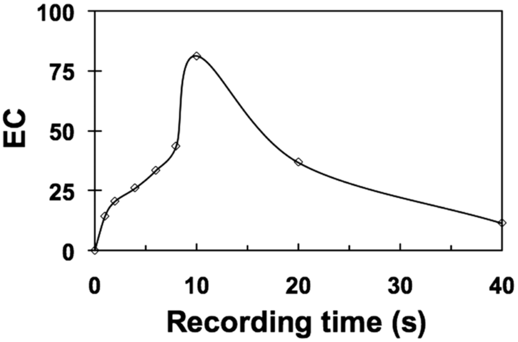

FIGURE 7 The EC of grating samples as a function of recording time. EC, the enhancement coefficient upon microphase separation.

increased quickly within 10 s to the maximum of about 81, and then decreased slowly. By changing the recording time, the EC can be controlled from 1 to 81, corresponding to the DE from 0.13% to 10%.

The three-dimensional (3D) AFM image of the grating samples revealed a direct change in surface relief before and after NSPS. Figure 6 shows the results of gratings recorded at 2 s, 10 s and 40 s, respectively. After recording, all the three samples exhibited sinusoidal curves in the 3D images with smooth profiles. Upon annealing, both higher amplitude and a little deformation owing to the enhancement were observed. Recorded at 2 s, the grating yielded a weak enhancement effect with an EC of about 14, resulting in a smaller surface deformation. Different from that, the grating recorded at 10 s displayed a seriously destroyed surface in its 3D AFM image. Since the maximum EC of about 81 was acquired, the larger deformation was ascribed to the stronger mass transportation in the NSPS process, which corresponds to the spoiled interface between bright and dark stripes in the POM images (Fig. 5). Grating recorded at a longer time (e.g., 40 s) exhibited a relatively smaller EC and a smaller deformation.

CONCLUSION

In the holographic gratings recorded in the ADLC P40A37, the first-order DE could be finely controlled by adjusting the recording time through the thermally-induced NSPS process. The optimized enhancement effect was obtained at 10-s recording, with the surface relief of about 120 nm and the first-order DE of about 10%. The maximum EC was 81, indicating that the ADLC materials have potential applications in secure information storage because the information cannot be easily read out without the finely controlled enhancement process.

REFERENCES

[1] Natansohn, A. & Rochon, P. (2002). *Chem. Rev.*, *102*, 4139.

[2] Viswanathan, N. K., Kim, D. Y., Bian, S. P., Williams, J., Liu, W., Li, L., Samuelson, L., Kumar, J., & Tripathy, S. K. (1999). *J. Mater. Chem.*, *9*, 1941.

[3] Ikeda, T. (2003). *J. Mater. Chem.*, *13*, 2037.

[4] Ikeda, T. & Tsutsumi, O. (1995). *Science*, *268*, 1873.

[5] Yamamoto, T., Hasagawa, M., Kanazawa, A., Shiono, T., & Ikeda, T. (1999). *J. Phys. Chem. B*, *103*, 9873.

[6] Stracke, A., Wendorff, J. H., Goldmann, D., Janietz, D., & Stiller, B. (2000). *Adv. Mater.*, *12*, 282.

[7] Zilker, S. J., Bieringer, T., Haarer, D., Stein, R. S., Egmond, J. W., & Kostromine, S. G. (1998). *Adv. Mater.*, *10*, 855.

[8] Zhao, Y., Bai, S., Asatryan, K., & Galstian, T. (2003). *Adv. Funct. Mater.*, *13*, 781.

[9] Fiore, G. D., Nicoletta, F. P., Macchione, M., Cupelli D., & Chidichimo, G. (2001). *Adv. Funct. Mater.*, *11*, 457.

[10] Zhao, Y. & Tong, X. (2003). *Adv. Mater.*, *15*, 1431.

[11] Ubukata, T., Seki, T., & Ichimura, K. (2000). *Adv. Mater.*, *12*, 1675.

[12] Tian, Y., Watanabe, K., Kong, X. X., Abe, J., & Iyoda, T. (2002). *Macromolecules*, *35*, 3739.

[13] Yu, H. F., Okano, K., Shishido, A., Ikeda, T., Kamata, K., Komura, M., & Iyoda, T. (2005). *Adv. Mater.*, *17*, 2184.

[14] Yu, H. F., Li, J. Z., Ikeda, T., & Iyoda, T. (2006). *Adv. Mater.*, *18*, 2213.

[15] Yu, H. F., Iyoda, T., & Ikeda, T. (2006). *J. Am. Chem. Soc.*, *128*, 11010.

[16] Yu, H. F., Iyoda, T., Okano, K., Shishido, A., & Ikeda, T. (2005). *Mol. Cryst. Liq. Cryst.*, *443*, 191.

[17] Yu, H. F., Shishido, A., Iyoda, T., & Ikeda, T. (2007). *Mol. Cryst. Liq. Cryst.*, *470*, 71.

[18] Barret, C. J., Rochon, P. L., & Natansohn, A. L. (1998). *J. Chem. Phys.*, *109*, 1505.

[19] Collier, R. J., Burckhardt, C. B., & Lin, L. H. (1971). *Optical Holography*, Academic Press: New York.

[20] Neff, V. D. (1974). Physico-chemical properties and methods of investigation. In: *Liquid Crystals and Plastic Crystals*, Gray, G. W. & Winsor, P. A. (Eds.), Ellis Horwood: U.K. Chichester, Vol. 2, 231–235.

[21] Weigert, F. (1919). *Verh. Dtsch. Phys. Ges.*, *21*, 485.